High-Mass SUSY Models at LHC and VLHC—Part I

I. Hinchliffe*
Lawrence Berkeley National Laboratory, Berkeley, CA
F.E. Paige†
Brookhaven National Laboratory, Upton, NY

Signatures are examined at VLHC and an very hihg luminosity LHC for SUSY models with large masses that consistent with existing constraints and having very heavy masses.

If supersymmetry is connected to the hierarchy problem, it is exptected that sparticles will be sufficiently light that at least some of them will be observable at the LHC [1]. As the sparticle masses rise, the fine tuning problem of the standard model reappears. However it is not possible to set a bound on the sparticle masses.

If SUSY is also the solution to the dark matter problem; the stable, lightest supersymmetric particle (LSP), being the particle that pervades the universe. This constraint can be applied to the minimal SUGRA [2] model to constrain the masses of the other sparticles. Recently minimal SUGRA points have been proposed [3] that satisfy existing constraints, including the dark matter constraint, but do not impose any fine tuning limits. This set of points is not a random sampling of the available parameter space. These points and their mass spectra are shown in Table I. Most of the allowed parameter space corresponds to the case where the sparticles have masses less than 1 TeV or so and is accessible to LHC. Indeed some of these points are quite similar to ones studied in earlier LHC simulations. Points A, B, C, D, E, G, J and L fall into this category. As the masses of the sparticles are increased, the LSP contribution to dark matter rises and typically violates the experimental constraints. However there are certain regions of parameter space where the annihilation rates for the LSP can be increased; in these narrow regions the sparticle masses can be much larger. Points F, K ,H and M illustrate these regions. This note considers Point K at at the LHC with a luminosity upgrade to $1000\,\mathrm{fb}^{-1}$ per year, (SLHC) and at a possible VLHC. We assume an energy of 40 TeV for the VLHC and use the identical analysis for both machines. Point L is considered in a companion note [4] and Point M in the group summary. Point F is similar to Point K except that the squark and slepton masses are much larger. For the purposes of this simulation, the detector performance at $10^{35}\,\mathrm{cm}^{-2}\mathrm{s}^{-1}$ is assumed to be the same as that of ATLAS for at the LHC design luminosity. In particular, the additional pileup is taken into account only by raising some of the cuts. In the So far, only the $t\bar{t}$, Wj, and Zj backgrounds have been included for the VLHC.

Point K has $M_A \approx 2M_{\tilde{\chi}_1^0}$ and gluino and squark masses above 2 TeV. The strong production is dominated by valance squarks, with $\tilde{q}_L \to \tilde{\chi}_1^{\pm}q, \tilde{\chi}_2^0 q$ and $\tilde{q}_R \to \tilde{\chi}_1^0 q$. The signal can be observed in the inclusive effective mass distribution. Events are selected with hadronic jets and missing E_T and the following scalar quantity formed

$$M_{\rm eff} = \not{E}_T + \sum_{\rm jets} E_{T,\rm jet} + \sum_{\rm leptons} E_{T,\rm lepton}$$

where the sum runs over all jets with $E_T > 50$ GeV and $|\eta| < 5.0$ and isolated leptons with $E_T > 15$ GeV and $|\eta| < 2.5$. The following further selection was then made: events were selected with at least two jets with $p_T > 0.1M_{\rm eff}$, $\not{E}_T > 0.3M_{\rm eff}$, $\Delta\phi(j_0, \not{E}_T) < \pi - 0.2$, and $\Delta\phi(j_0, j_1) < 2\pi/3$. These cuts help to optimize the signal to background ratio. The distributions in this variable for signal and background are shown in 1. It can be seen that the signal emerges from the background at large values of $M_{\rm eff}$. The LHC signal with 3000 fb^{-1} of integrated luminosity has a signal of 510 events on a background of 108 for $M_{\rm eff} > 4000$ GeV. These rates are sufficiently large so that a discovery could be made with the standard integrated luminosity of 300 fb^{-1}.

*I_Hinchliffe@lbl.gov
†paige@bnl.gov

Table I Benchmark SUGRA points and masses from [3]

Model	A	B	C	D	E	F	G	H	I	J	K	L	M
$m_{1/2}$	600	250	400	525	300	1000	375	1500	350	750	1150	450	1900
m_0	140	100	90	125	1500	3450	120	419	180	300	1000	350	1500
$\tan\beta$	5	10	10	10	10	10	20	20	35	35	35	50	50
sign(μ)	+	+	+	−	+	+	+	+	+	+	−	+	+
$\alpha_s(m_Z)$	120	123	121	121	123	120	122	117	122	119	117	121	116
m_t	175	175	175	175	171	171	175	175	175	175	175	175	175
Masses													
h^0	114	112	115	115	112	115	116	121	116	120	118	118	123
H^0	884	382	577	737	1509	3495	520	1794	449	876	1071	491	1732
A^0	883	381	576	736	1509	3495	520	1794	449	876	1071	491	1732
$H^\pm$	887	389	582	741	1511	3496	526	1796	457	880	1075	499	1734
χ_1^0	252	98	164	221	119	434	153	664	143	321	506	188	855
χ_2^0	482	182	310	425	199	546	291	1274	271	617	976	360	1648
χ_3^0	759	345	517	654	255	548	486	1585	462	890	1270	585	2032
χ_4^0	774	364	533	661	318	887	501	1595	476	900	1278	597	2036
$\chi_1^\pm$	482	181	310	425	194	537	291	1274	271	617	976	360	1648
$\chi_2^\pm$	774	365	533	663	318	888	502	1596	478	901	1279	598	2036
$\tilde{g}$	1299	582	893	1148	697	2108	843	3026	792	1593	2363	994	3768
e_L, μ_L	431	204	290	379	1514	3512	286	1077	302	587	1257	466	1949
e_R, μ_R	271	145	182	239	1505	3471	192	705	228	415	1091	392	1661
ν_e, ν_μ	424	188	279	371	1512	3511	275	1074	292	582	1255	459	1947
τ_1	269	137	175	233	1492	3443	166	664	159	334	951	242	1198
τ_2	431	208	292	380	1508	3498	292	1067	313	579	1206	447	1778
ν_τ	424	187	279	370	1506	3497	271	1062	280	561	1199	417	1772
u_L, c_L	1199	547	828	1061	1615	3906	787	2771	752	1486	2360	978	3703
u_R, c_R	1148	528	797	1019	1606	3864	757	2637	724	1422	2267	943	3544
d_L, s_L	1202	553	832	1064	1617	3906	791	2772	756	1488	2361	981	3704
d_R, s_R	1141	527	793	1014	1606	3858	754	2617	721	1413	2254	939	3521
t_1	893	392	612	804	1029	2574	582	2117	550	1122	1739	714	2742
t_2	1141	571	813	1010	1363	3326	771	2545	728	1363	2017	894	3196
b_1	1098	501	759	973	1354	3319	711	2522	656	1316	1960	821	3156
b_2	1141	528	792	1009	1594	3832	750	2580	708	1368	2026	887	3216

Production of $\tilde{q}_R\tilde{q}_R$ followed by the decay of each squark to $q\tilde{\chi}_1^0$ gives a dijet signal accompanied by missing E_T. In order to extract this from the standard model background, hard cuts on the jets and $\not{E}_T$ are needed. Events were required to have two jets with $p_T > 700$ GeV, $\not{E}_T > 600$ GeV, and $\Delta\phi(j_1, j_2) < 0.8\pi$. The resulting distributions are shown in Figure 2. Only a few events survive at the LHC with 3000 fb^{-1}. The transverse momentum of the hardest jet is sensitive to the $\tilde{q}_R$ mass[5].

The decay $\tilde{\chi}_2^0 \to \tilde{\chi}_1^0 h$ is dominant so we should expect to see Higgs particles in the decay of $\tilde{q}_L$ ($\tilde{q}_L \to \tilde{\chi}_2^0 q \to \tilde{\chi}_1^0 hq$). The Higgs signal should be observed as a peak in the $b\bar{b}$ mass distributions. There is a large background from $t\bar{t}$ that must be overcome. Events were selected to have at least three jets with $p_T > 600, 300, 100$ GeV, $\not{E}_T > 400$ GeV, $M_{\text{eff}} > 2500$ GeV, $\Delta\phi(j_1, \not{E}_T) < 0.9\pi$, and $\Delta\phi(j_1, j_2) < 0.6\pi$. The distributions are shown in Figure 3 assuming the same b-tagging performance as for standard luminosity, i.e., that shown in Figure 9-31 of Ref. [5] which corresponds to an efficiency of 60% and a rejection factor against light quark jets of ~ 100. This b-tagging performance may be optimistic in the very high luminosity environment. However our event selection is only $\sim 10\%$ efficient at SLHC and might be improved. There is much less standard model background at VLHC. Here there is significant SUSY background from $\tilde{g} \to \tilde{b}_i\bar{b}, \tilde{t}_1\bar{t}$.

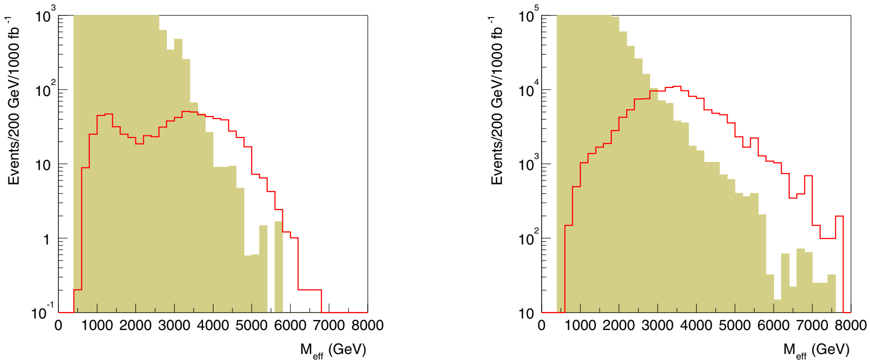

Figure 1: $M_{\rm eff}$ distribution for SLHC (left) and VLHC (right) for Point K. Solid: signal. Shaded: SM background.

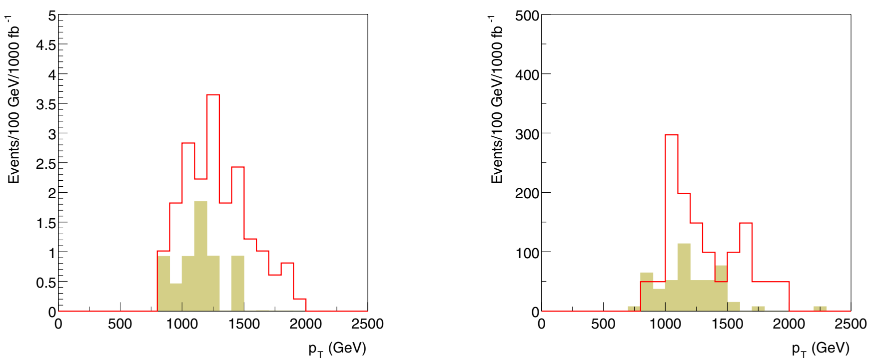

Figure 2: p_T distribution of hardest jet in 2jet + $\not\!\!E_T$ events for SLHC (left) and VLHC (right) for Point K.

While the masses of the sparticles at Point K are such that SUSY would be discovered at the baseline LHC, the event rates are small and detailed SUSY studies will not be possible. The reach of the LHC for would be improved by higher luminosity where the extraction of specific final states will become possible. The cross section at a 40 TeV VLHC is approximately 100 times larger than that at LHC. This leads to a substantial gain, but it is important to emphasize that this gain requires luminosity at least as large as that ultimately reached by the LHC and detectors capable of exploiting it.

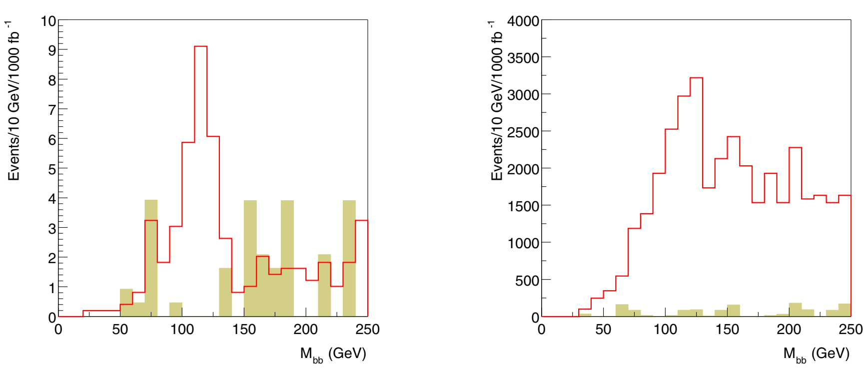

Figure 3: M_{bb} distribution for SLHC (left) and VLHC (right) for Point K.

The work was supported in part by the Director, Office of Energy Research, Office of High Energy and Nuclear Physics of the U.S. Department of Energy under Contracts DE–AC03–76SF00098 and DE-AC02-98CH10886. Accordingly, the U.S. Government retains a nonexclusive, royalty-free license to publish or reproduce the published form of this contribution, or allow others to do so, for U.S. Government purposes.

References

[1] G. W. Anderson and D. J. Castano, Phys. Lett. B **347**, 300 (1995). R. Barbieri and G. F. Giudice, Nucl. Phys. B **306**, 63 (1988).
[2] L. Alvarez-Gaume, J. Polchinski and M.B. Wise, Nucl. Phys. **B221**, 495 (1983); L. Ibañez, Phys. Lett. **118B**, 73 (1982); J.Ellis, D.V. Nanopolous and K. Tamvakis, Phys. Lett. **121B**, 123 (1983); K. Inoue *et al.* Prog. Theor. Phys. **68**, 927 (1982); A.H. Chamseddine, R. Arnowitt, and P. Nath, Phys. Rev. Lett., **49**, 970 (1982).
[3] M. Battaglia *et al.*, hep-ph/0106204.
[4] I. Hinchliffe and F. E. Paige (in preparation)
[5] ATLAS Collaboration, *ATLAS Detector and Physics Performance Technical Design Report*, CERN/LHCC/99-14, `http://atlasinfo.cern.ch/Atlas/GROUPS/PHYSICS/TDR/-access.html`.